Spatial Stability Analysis of Chevron Jet Profiles*

Kristjan Gudmundsson† and Tim Colonius‡
California Institute of Technology, Pasadena, CA, 91125, U.S.A.

We investigate the linear stability characteristics of mean flows produced by round, and chevron nozzles. We derive a Rayleigh equation for the chevron profile, which allows the fast solution of the chevron stability problem. Using PIV and RANS data, we compute the stability characteristics of various chevron/round nozzles. We find there are two main differences between the chevron and round jet: chevron jet growth rates are highly suppressed and peak growth rates shifted to lower frequencies, and phase speeds are somewhat increased. Some preliminary implications on sound generation are discussed. We compare our instability wave results to microphone measurements taken with a phased hydrodynamic array. Our results indicate that the hydrodynamic pressure field of both round, and chevron jets is consistent with that of the instability modes of the turbulent, spreading mean flow.

Introduction

Apart from increasing turbofan bypass ratios, different approaches to noise reduction have been pursued, including the machining of serrations, or chevrons, into the nozzle lip (Fig. 1). The chevrons generate streamwise vortices that enhance mixing and shorten the potential core. They also reduce noise at low frequencies and aft angles, but increase noise at high frequencies. The high frequency penalty may be associated with the increased levels of small scale turbulence, while the noise reduction at lower frequencies, associated with the large scale structures of the flow, is not well understood. Sound radiated at aft-angles/low-frequencies has typically been associated with large-scale structures of the flow, which are in turn related to instabilities of the inflectional mean velocity profile (Crighton & Gaster,[1] Mankbadi & Liu[2]), while recent work (Goldstein & Leib[3]) shows linear instabilities to be important in sound generation at aft angles and low frequencies. It thus seems that the chevron effect on the far-field noise at aft-angles/low-frequencies is, at least in part, due to their moderation of the large-scale structures of the flow.

At present, the design and deployment of chevron nozzles is based on empirical laboratory, and full-scale testing. Due to the complexity of the near-nozzle flow field, there are currently no physics-based prediction methods for noise reduction; properly resolving the large-scale flow structures is difficult, even with modeling tools such as Large Eddy Simulation. As a surrogate, we propose to compute the linear instability modes of the time-averaged chevron flow field, and to investigate the extent to which the chevrons modify the stability characteristics of an equivalent-thrust round jet.

Linear stability analysis on quasi-parallel flows assumes a negligible spread rate over typical fluctuation length-scales, so that cross sections of the jet (Fig. 1) are analyzed as if each one was a sample from an unbounded parallel mean flow. This approach was applied to planar shear layers by e. g. Michalke,[4] and to round jets by e. g. Batchelor & Gill,[5] Mattingly & Chang,[6] and more recently by Suzuki & Colonius,[7] who showed the hydrodynamic pressure field of a round jet to be consistent with that of the instability modes of the spreading mean flow, even for unforced, fully turbulent jets.

*Work supported by an AeroAcoustics Research Consortium (AARC) grant from the Ohio Aerospace Institute (OAI)
†Ph.D. Candidate, Department of Mechanical Engineering, Student Member AIAA
‡Professor, Department of Mechanical Engineering, Member AIAA

The appropriateness of the quasi-parallel assumption for the chevron jet is analyzed as follows. The potential core length for the chevrons we consider here is shorter than the round jet by about 2 diameters (Bridges & Brown[8]). This corresponds to an increase in (azimuthally averaged) spread rate from about 0.18 for the straight nozzle to about 0.25 for the chevron nozzle. Thus the assumption of locally parallel mean flow is somewhat less appropriate for the chevron jet, but still reasonable as a first approximation.

Standard quasi-parallel stability analysis of jet flows considers, at each streamwise position, a one-dimensional (ordinary differential) eigenvalue problem in the cross flow direction, and is amenable to direct matrix solution or shooting algorithms. The chevron jet, on the other hand, is inhomogeneous in both coordinate directions normal to the stream (see Fig. 1), and so forms a two-dimensional (partial differential) eigenvalue problem. As such it is more computationally intensive than the one-dimensional problem.

Chevron stability characteristics were studied in our previous work (Gudmundsson & Colonius[9]), where a high-order accurate Navier-Stokes (NS) solver was coupled with the iterative eigensystem solver ARPACK, using PIV mean flow data from Bridges & Brown.[8] Due to the high computational expense of the NS-ARPACK solver, this study was limited to two chevron designs, at a single cross section, $x/D = 2$ (cold, $M = 0.9$ jet). There are two common approaches to the stability problem: the *temporal* approach, where disturbances are assumed to grow in time, but not in space; and the *spatial* approach, where disturbances are assumed to grow in the flow direction, but not in time (at fixed observation points). The latter approach seems more apropos to the convectively unstable flow in question, and indeed has been more successful upon comparison to experiments (Huerre & Monkewitz[10]). As discussed in our previous study,[9] the spatial approach results in a singular, non-linear eigenvalue problem, while the temporal problem is well-conditioned, and linear. We thus solved the temporal problem, in order to gain insight into the spatial problem (the two approaches can be approximately related through the Gaster[11] transform). Upon analysis of the results obtained in our previous study, we discovered that the chevron jet stability modes obey certain symmetries. Using these symmetries, we have obtained a Rayleigh equation (Eqn. (7)) for the chevron jet, which can be solved in either temporal, or spatial mode. In addition, this new approach is up to four orders of magnitude faster than our previous NS-ARPACK solver. The key observation here is that a chevron nozzle having N_c chevrons will produce a mean flow-field having N_c-fold azimuthal symmetry. As an example, when $N_c = 6$, the mean flow-field will only contain azimuthal modes in multiples of six. This places significant limitations on the solution to the stability problem. Applying these constraints transforms the 2D PDE problem to a system of ODEs, allowing us to obtain the solution at a fraction of the cost of the NS-ARPACK solver, which searches amongst all solutions satisfying the linearized NS-equations.

Computational Method

We linearize the flow (assumed to be governed by the Euler equations, non-dimensionalized by the jet diameter D, ambient sound speed a_∞ and ambient density ρ_∞) around a quasi-parallel mean flow described by

$$\overline{q}(r,\theta) = [\overline{U}(r,\theta), 0, 0, \frac{1}{\gamma}],$$

where γ is the ratio of specific heats, and we are neglecting mean thermal gradients. The jets considered in this study have a temperature ratio of $T_{jet}/T_\infty = 0.96$, so that some mean temperature gradients exist, but as a first approximation we leave these out. Under the quasi-parallel flow assumption, the solution $q^*(r,\theta,x,t) = [u_x^*, u_r^*, u_\theta^*, p^*]$ will be wavelike in both the flow direction, x, and time, t:

$$q^*(r,\theta,x,t) = q(r,\theta)\, e^{i(kx-\omega t)} + \text{c.c.}, \tag{1}$$

where $k = k_r + ik_i$ and $\omega = \omega_r + i\omega_i$, and c.c. denotes the complex conjugate. k_r and ω_r denote wavenumber and frequency, respectively, while k_i and ω_i denote spatial and temporal growth rates, respectively. If $\omega_i > 0$, disturbances will grow in time t, and if $k_i < 0$, disturbances will grow in flow direction x. In the temporal approach, we assume $k_i = 0$, and search for temporally unstable solutions, while in the spatial approach, we assume $\omega_i = 0$, and search for spatially unstable solutions.

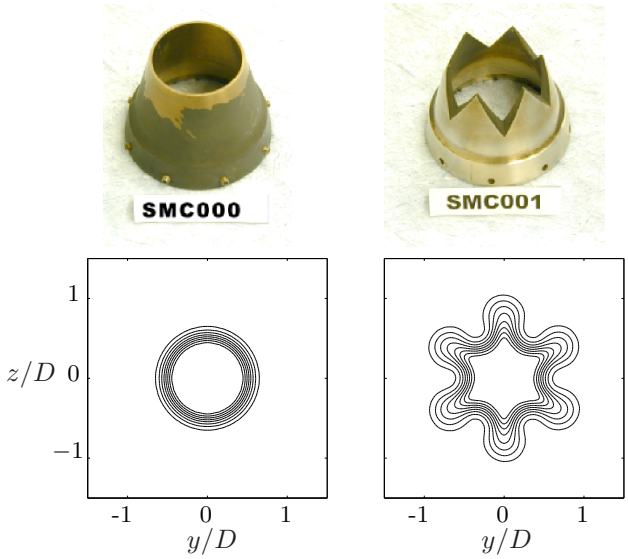

Figure 1. The two nozzles (top) used in this study, and their respective mean flows $\overline{U}(r,\theta)$ (bottom), at $x/D = 2$. Serial numbers `SMC000` and `SMC001` are as defined by Bridges et. al.[8]

Eliminating all variables but pressure, we obtain

$$\frac{1}{r}\frac{\partial}{\partial r}\left(r\frac{\partial p}{\partial r}\right) - \frac{2k}{k\overline{U}-\omega}\frac{\partial \overline{U}}{\partial r}\frac{\partial p}{\partial r} - \frac{2k}{r^2(k\overline{U}-\omega)}\frac{\partial \overline{U}}{\partial \theta}\frac{\partial p}{\partial \theta} + \frac{1}{r^2}\frac{\partial^2 p}{\partial \theta^2} - \left(k^2 - (k\overline{U}-\omega)^2\right)p = 0. \tag{2}$$

Taking the azimuthal Fourier transform of this equation, (letting T_n denote the n-th Fourier coefficient of quantity T), we obtain

$$\frac{1}{r}\frac{d}{dr}\left(r\frac{dp_m}{dr}\right) + \sum_{n=-\infty}^{\infty}\left(F_n\frac{d}{dr} + (m-n)\,G_n + H_n\right)p_{m-n} - \left(\frac{m^2}{r^2}+k^2\right)p_m = 0, \tag{3}$$

where

$$F_j = -2k\left(\frac{1}{k\overline{U}-\omega}\frac{\partial \overline{U}}{\partial r}\right)_j, \tag{4}$$

$$G_j = -\frac{2ik}{r^2}\left(\frac{1}{k\overline{U}-\omega}\frac{\partial \overline{U}}{\partial \theta}\right)_j, \tag{5}$$

$$H_j = \left(k\overline{U}-\omega\right)_j^2. \tag{6}$$

For arbitrary mean flow profiles $\overline{U}(r,\theta)$, we thus have an infinite-dimensional system of ODEs to solve. However, chevron profiles are special in that they possess azimuthal symmetries, such that only mode-numbers in multiples of the chevron count N_c will be non-zero. This drastically simplifies the convolutions described by equations (4) through (6), in that $F_j = 0$ if $j \neq N_c l$, where l is any integer, and similarly for G_j and H_j. Upon truncation of the infinite summation in Eqn. (3), we obtain the *Compressible Rayleigh Equation* (CRE) *for a chevron nozzle with N_c chevrons:*

$$\frac{1}{r}\frac{d}{dr}\left(r\frac{dp_m}{dr}\right) + \sum_{n=-N}^{N}\left(F_{N_c n}\frac{d}{dr} + (m-N_c n)\,G_{N_c n} + H_{N_c n}\right)p_{m-N_c n} - \left(\frac{m^2}{r^2}+k^2\right)p_m = 0, \tag{7}$$

whose solution forms

$$p(r,\theta) = \sum_{n=-N}^{N} p_{m-N_c m}(r)\, e^{i(m-N_c n)\theta}, \tag{8}$$

where N, the summation limit, depends on the mean flow $\overline{U}(r,\theta)$. In our experience, $N = 2$ is sufficient to capture essential solution features. As is evident from the chevron CRE, the lobes of the chevron nozzle couple certain instability modes. As an example, consider the case where $m = 0$, and $N_c = 6$: p_0 will be dependent upon p_{-6}, p_6 and so on. We note that when the mean flow $\overline{U}(r,\theta)$ is axisymmetric (i. e. $\overline{U}(r,\theta) = \overline{U}(r)$), the chevron CRE reduces to the familiar round-jet CRE:

$$\frac{1}{r}\frac{d}{dr}\left(r\frac{dp_m}{dr}\right) - \frac{2k}{k\overline{U}-\omega}\frac{d\overline{U}}{dr}\frac{dp_m}{dr} - \left(\frac{m^2}{r^2} + k^2 - (k\overline{U}-\omega)^2\right)p_m = 0. \tag{9}$$

As $r \to 0$, and $r \to \infty$, the modes become uncoupled, each of them independently obeying the round-jet CRE, Eqn. (9), with a homogeneous mean flow term:

$$\frac{1}{r}\frac{d}{dr}\left(r\frac{dp_m}{dr}\right) - \left(\frac{m^2}{r^2} + k^2 - (k\overline{U}-\omega)^2\right)p_m = 0. \tag{10}$$

Eqn. (10) is the Bessel equation, whose solutions are the Bessel functions of the first and second kind, and linear combinations thereof. The boundary conditions for the chevron CRE follow from this,

$$\text{as } r \to 0 \qquad p_m(r) \sim J_m(\sqrt{(\omega-k)^2 - k^2}\, r), \tag{11}$$

and

$$\text{as } r \to \infty \qquad p_m(r) \sim H_m^2(\sqrt{w^2 - k^2}\, r), \tag{12}$$

where J_m and H_m^2 are the m-th order Bessel function of the first kind, and Hankel function of the second kind, respectively. The chevron CRE, Eqn. (7), along with boundary conditions, Eqns. (11) and (12), forms a two-point boundary value problem, solvable via the shooting method.

The above was implemented in MATLAB$^{\text{TM}}$, and validated using the NS-ARPACK solver, which in turn was independently validated as described in our previous study.[9]

Experimental Data

Three separate datasets are used in this study. Mean flow data for the round nozzle (`SMC000`) was obtained from time-averaged PIV measurements conducted by Bridges et al,[8] in the Small Hot Jet Acoustic Rig (depicted in Fig. 2), at the NASA Glenn Research Center. PIV mean flow data for the chevron nozzle (`SMC001`) is not available for the flow conditions analyzed in this study ($M = 0.5$, $T_{jet}/T_\infty = 0.96$ and $Re = 7{\cdot}10^5$) ; this was obtained via RANS calculations performed by the Thaerocomp Technical Corp. (TTC). The microphone data was obtained from the Phased Hydrodynamic Array (also shown in Fig. 2) at the SHJAR. This array consists of thirteen concentric rings, each carrying six microphones. More details on the experimental setup can be found in Suzuki & Colonius.[7]

Results

Growth Rates and Eigenfunctions

Fig. 3 shows eigenfunctions $Re[p(r,\theta)]$ for $m = 0$ and 1, corresponding to $St = 0.5$ at $x/D = 0$. As is clear from these figures, the chevron eigenfunction corresponding to $m = 0$ is not actually axisymmetric, as the $m = 0$ designation implies. However, this chevron mode has a direct correspondence with the axisymmetric mode of the round jet. This can be seen by inspection of the chevron CRE; letting the off-diagonal terms

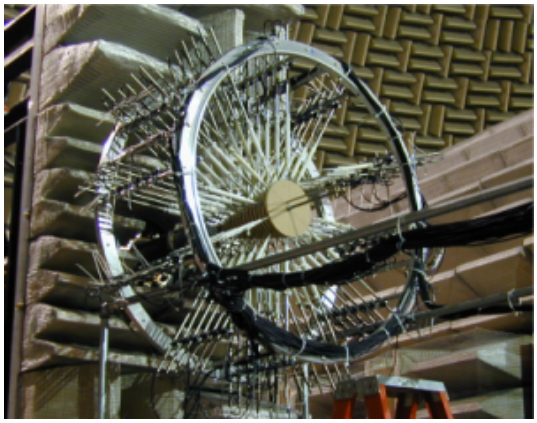

Figure 2. The Small Hot Jet Acoustic Rig (SHJAR) and Hydrodynamic Array at the NASA Glenn Research Center.

F_n, G_n and H_n, $n \neq 0$, go to zero will recover the round jet CRE for $m = 0$, and similarly for $m = 1$ etc. This analysis thus reveals how the chevrons impact and deform the respective round jet modes.

Fig. 4 shows maximal growth rates $\max_{St}(-k_i D)$, and corresponding phase speeds $c_p = \omega/(k_r a_\infty)$ and Strouhal numbers $St = \omega D/(2\pi U_{jet})$ vs axial position x/D, for $m = 0$ and 1, for nozzles `SMC000` and `SMC001`. The most prominent feature in these figures is the degree to which the chevron growth rates and phase speeds are suppressed and increased, respectively, as compared to those of the thrust-equivalent round nozzle. Fig. 5 illustrates the spatial evolution of the amplification factor, $A(x)$, defined as

$$A(x) = \exp\left(i \int^x k(\xi)\, d\xi\right), \tag{13}$$

where $k(\xi)$ represents the eigenvalue (growth rate and wavenumber) computed at axial location ξ. The amplification factor defines the envelope in which the instability waves grow, and subsequently decay as the jet shear-layer spreads. These figures again illustrate the retarded growth of chevron instability waves, as compared to that of the round jet. The chevron waves also have higher spatial wavenumbers ($k_r = Re[k]$), resulting in faster oscillations in the flow direction. In our previous study,[9] we solved the temporal stability problem, for two chevron jets and a round jet. We note that, despite the previous study being in the temporal context and limited to a single cross-section, our previous results are consistent with the findings of the current study, in that we again find that chevron growth rates are suppressed, and phase speed increased, as compared to that of the round nozzle.

Sound radiated from jets at shallow angles and low frequency has typically been associated with large-scale structures that are in turn related to instabilities of the inflection mean velocity profile.[1,2] Qualitative[12–14] and quantitative analysis[15] connect the envelope and phase speed of instability waves with the acoustic efficiency and directivity at these aft angles. Here we do not attempt any detailed comparison between the instability results and acoustic far field for the chevron jets. However, some observations based on the data are appropriate. First, we observe a suppression of growth rate that is consistent with low frequency noise reductions between the nozzles. That is, the high penetration chevrons that have the highest low frequency noise suppression also have the lowest growth rates. Another important aspect of the acoustic efficiency of wave packets is their phase speed: the closer to sonic (with respect to ambient), the higher the radiation. As Fig. 4 shows, the chevron instability waves have phase speeds that increase by as much as 20% for $m = 0$, and 10% for $m = 1$, compared to the circular nozzle. While a firm conclusion awaits a more detailed analysis, it would appear that the growth rate suppression is the more significant effect.

Comparison With Microphone Data

As described above, each ring in the hydrodynamic array carries six microphones, so that a certain degree of aliasing of higher modes is to be expected for the chevron jet. As an example, modes in multiples of six will all be aliased (added) onto mode $m = 0$, so that

$$p_{measured}(m = 0) = \sum_{n=-\infty}^{\infty} p_{actual}(m = 6n). \tag{14}$$

To compare our computational results to the microphone data, we mimic aliasing by setting e.g.

$$\hat{p}_0(r) = p_0(r) + p_{-6}(r) + p_6(r), \tag{15}$$

and then use $\hat{p}_0$ for comparison. To approximately account for the spreading of the mean flow, we define the *global* (and aliased) instability wave as

$$P(x, r, m) = \hat{p}(r, m|x)\ e^{i \int^x k(\xi)\, d\xi}, \tag{16}$$

where $\hat{p}(r, m|x)$ and $k(x)$ represent the solution to the stability problem at axial location x. Here, $\hat{p}(r, m|x)$ has been normalized such that $\max_r |\hat{p}(r, m|x)| = 1$. The global instability wave is, of course, arbitrarily normalized, but the amplitude and phase at the nozzle exit, a_i, say, can be estimated using the microphone data. This data is available at discrete locations $P_{mic}(x_j, r_j, m)$, so that a least-squares estimate of a_i can be obtained via the minimization of

$$J(a_i) = \sum_{j=1}^{n_{mic}} \left(P_{mic}(x_j, r_j, m) - a_i P(x_j, r_j, m)\right)^2, \tag{17}$$

resulting in

$$a_i = \frac{\sum_{j=1}^{n_{mic}} P_{mic}(x_j, r_j, m)\, P(x_j, r_j, m)}{\sum_{j=1}^{n_{mic}} P(x_j, r_j, m)^2}. \tag{18}$$

Fig. 6 shows $a_i(m, St)$ for both the round, and chevron nozzle. Initial amplitude levels are considerably higher for the chevron jet. This is due to the higher levels of turbulence at the chevron exit, and the higher chevron spread rate. The higher spread rate results in the microphones being in greater proximity to the turbulent shear layer, resulting in higher pressure levels, and hence higher estimated initial amplitudes. The latter effect also explains the jagged nature of the chevron microphone data. The microphone rings are arranged such that microphones on adjacent rings are rotated by 30 degrees in order to minimize aliasing. Thus, when the microphones are next to the chevron fingers, a higher pressure value is recorded, and vice versa, explaining the up-down pressure jumps between data points. This is schematically illustrated in Fig. 11.

Figs. 7 and 8 show comparisons between microphone data and the global eigenfunctions described above for the round nozzle, for a range of Strouhal numbers. The fit obtained in this case suggests, as previously discussed by Suzuki & Colonius,[7] that the hydrodynamic pressure field of a round jet is consistent with that predicted by the instability waves of the turbulent mean flow. We note that the fit improves with increasing Strouhal number. This is due to non-parallel effects; with increasing frequency, disturbance wavelengths become progressively smaller so that the mean flow is effectively locally-parallel (i.e. the mean flow does not change much over the disturbance wavelength). Also, the fit is better for $m = 1$ than for $m = 0$. This is also a non-parallel effect; mode $m = 0$ scales with the diameter of the jet, while all other modes scale with the shear-layer thickness. This is due to boundary condition at the jet axis; $p_0(0) = 1$, while $p_m(0) = 0$ when $m \neq 0$.

Figs. 9 and 10 show similar results for the chevron nozzle. The fit obtained in this case indicates that instability waves play a similar role in the chevron hydrodynamic pressure field, as they do for round nozzles. This in turn suggests that instability wave calculations can provide approximate indicators of chevron performance. Our approach allows the fast computation (on the order of minutes) of these stability characteristics and hence could prove a valuable tool in improving nozzle designs, based on physical principles.

Conclusions

We have derived a generalized Rayleigh equation (Eqn. (7)) that governs the quasi-parallel stability modes for both round, and chevron jets. We have implemented this equation, obtaining an algorithm for the fast solution of the chevron/round jet spatial/temporal stability problem. This algorithm is up to four orders of magnitude faster than our previous NS-ARPACK solver, which is also limited to the temporal problem, but has the advantage of accepting arbitrary mean flow profiles. Using experimental PIV data from the SHJAR at the NASA Glenn Research Center, as well RANS data from the Thaerocomp Technical Corp., we have computed the stability characteristics of various chevron/round nozzles. There are two main differences between the chevron and round jet: growth rates are highly suppressed while peak growth rates are shifted to lower frequencies, and phase speeds are somewhat increased. While a firm conclusion awaits a more detailed analysis, it would appear that the growth rate suppression is the most significant effect. In our previous study,[9] we solved the temporal stability problem, for two chevron jets and a round jet. We note that–despite the previous study being in the temporal context and limited to a single cross-section–our previous results are consistent with the findings of the current study, in that we again find that chevron growth rates are suppressed, and phase speed increased, as compared to that of the round nozzle.

We compare the evolution of the computed instability waves with data from a caged 78 microphone array tested in SHJAR. The microphones were placed on a conical surface just outside the jet shear layers and resolved azimuthal modes $m = 0$, $m = \pm 1$, and $m = \pm 2$. The fit obtained for the round nozzle is in agreement with the previous work by Suzuki & Colonius.[7] The fit obtained for the chevron nozzle is similarly promising, which suggests that instability wave calculations can provide approximate, but important indicators of chevron performance. Our approach allows the fast computation of these stability characteristics and hence could prove a valuable tool in improving nozzle designs, based on physical principles.

Acknowledgments

The authors acknowledge the support of an AeroAcoustics Research Consortium (AARC) grant from the Ohio Aerospace Institute (OAI). We would like to express great appreciation to Dr. James Bridges and colleagues at the NASA Glenn Research Center for collecting and providing us with their data, and to the Thaerocomp Technical Corp. for performing RANS computations on the `SMC001` nozzle. In addition, we would like to thank Dr. Cyrille Breard for pointing out an error in an earlier formulation of Eqn. (2).

References

[1]Crighton, D. G. and Gaster, M., "Stability of Slowly Diverging Jet Flow," *J. Fluid Mech.*, Vol. 77, 1976, pp. 397–413.

[2]Mankbadi, R. and Liu, J. T. C., "A Study of the Interactions Between Large-Scale Coherent Structures and Fine-Grained Turbulence in a Round Jet," *Proc. Roy. Soc. London*, Vol. 1443, 1981, pp. 541–602.

[3]Goldstein, M. and Leib, S., "The role of instability waves in predicting jet noise," *J. Fluid Mech.*, Vol. 525, 2005, pp. 37–72.

[4]Michalke, A., "On the inviscid instability of the hyperbolic-tangent velocity profile," *J. Fluid Mech.*, Vol. 19(4), 1964.

[5]Batchelor, G. K. and Gill, A. E., "Analysis of the stability of axisymmetric jets," *J. Fluid Mech.*, Vol. 14(4), 1962, pp. 529–551.

[6]Mattingly, G. E. and Chang, C. C., "Unstable waves on an axisymmetric jet column," *J. Fluid Mech.*, Vol. 63(3), 1974, pp. 541–560.

[7]Suzuki, T. and Colonius, T., "Instability waves in a subsonic round jet detected using a near-field phased microphone array," *J. Fluid Mech.*, Vol. In Press, 2006.

[8]Bridges, J. and Brown, C. A., "Parametric testing of chevrons on single flow hot jets," *AIAA J.*, Vol. 2004-2824, 2004.

[9]Gudmundsson, K. and Colonius, T., "Linear Stability Analysis of Chevron Jet Profiles," ASME Joint U. S. -European Fluids Engineering Summer Meeting, Miami, 17 - 20 July 2006.

[10]Huerre, P. and Monkewitz, P. A., "Local and global instabilities in spatially developing flows," *Annu. Rev. Fluid Mech.*, Vol. 22, 1990, pp. 437–537.

[11]Gaster, M., "A note on the relation between temporally-increasing and spatially-increasing disturbances in hydrodynamic stability," *J. Fluid Mech.*, 1962, pp. 222–224.

[12]Crighton, D. G. and Huerre, P., "Shear-Layer Pressure-Fluctuations and Superdirective Acoustics Sources," *J. Fluid Mech.*, Vol. 220, 1990, pp. 355–368.

[13]T. Colonius, S. K. L. and Moin, P., "Sound generation in a mixing layer," *J. Fluid Mech.*, Vol. 330, 1997, pp. 375–409.

[14]Freund, J., "Noise sources in a low-Reynolds-number turbulent jet at Mach 0.9," *J. Fluid Mech.*, Vol. 438, 2001, pp. 277–305.

[15]R. Reba, S. Narayanan, T. C. and Dunlop, M., "A Study of the Role of Organized Structures in Jet Noise Generation," *AIAA Paper 2003-3314*, 2003.

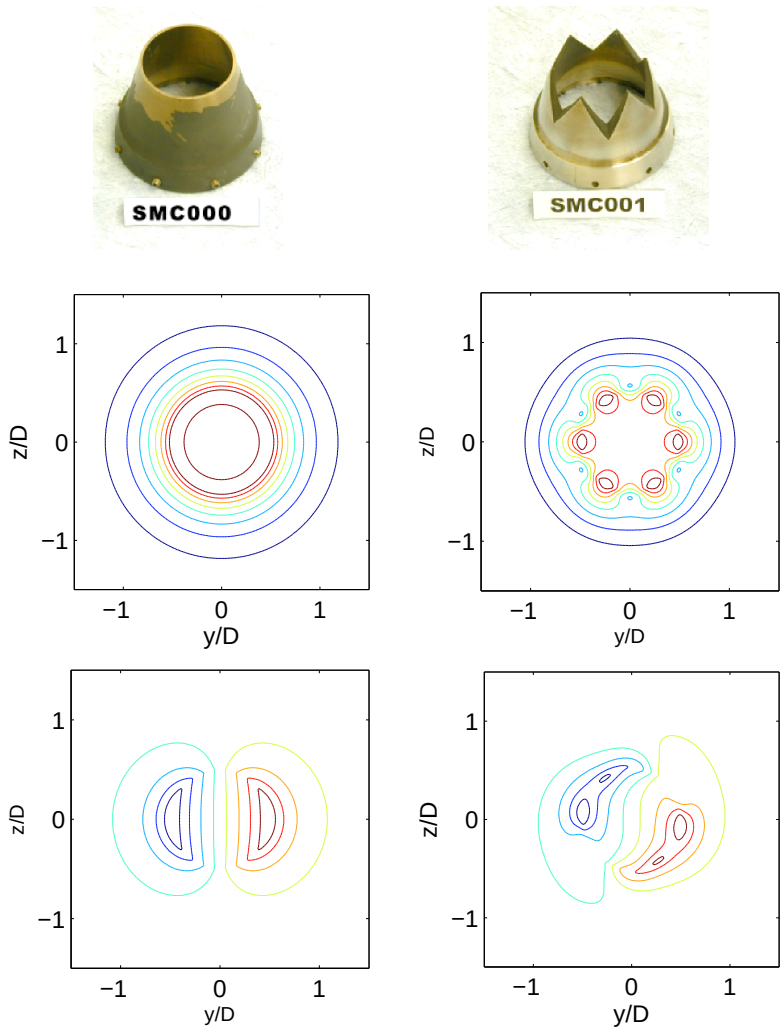

Figure 3. Eigenfunctions $Re[p(r,\theta)]$ **for** $m = 0$ **(top) and** $m = 1$ **(bottom), with** $St = \omega D/(2\pi U_{jet}) = 0.5$ **and** $M = 0.5$ **at** $x/D = 0$**.**

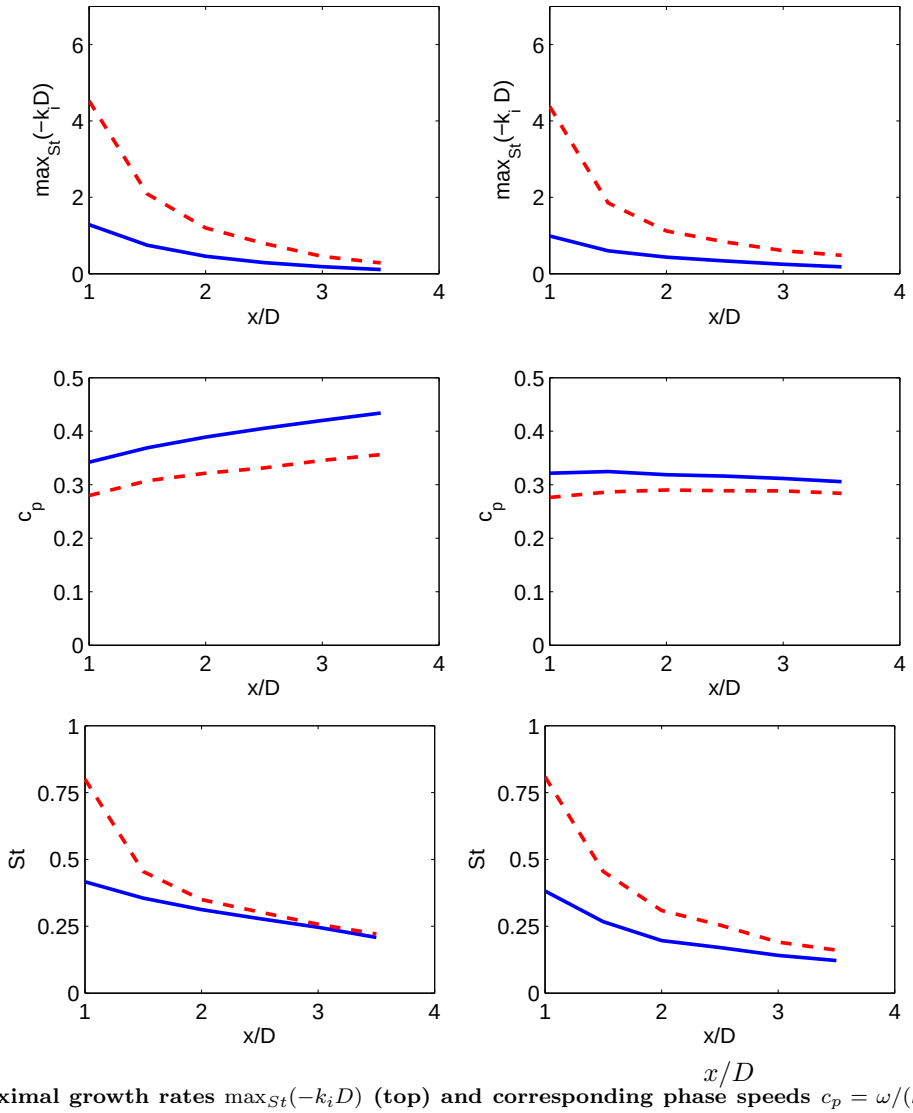

Figure 4. Maximal growth rates $\max_{St}(-k_i D)$ **(top) and corresponding phase speeds** $c_p = \omega/(k_r a_\infty)$ **(middle) and Strouhal numbers** $St = \omega D/(2\pi U_{jet})$ **(bottom), vs axial position** x/D**. Left/Right:** $m = 0/m = 1$**. Round nozzle** `SMC000`(- - - -)**, chevron nozzle** `SMC001`(———)**.**

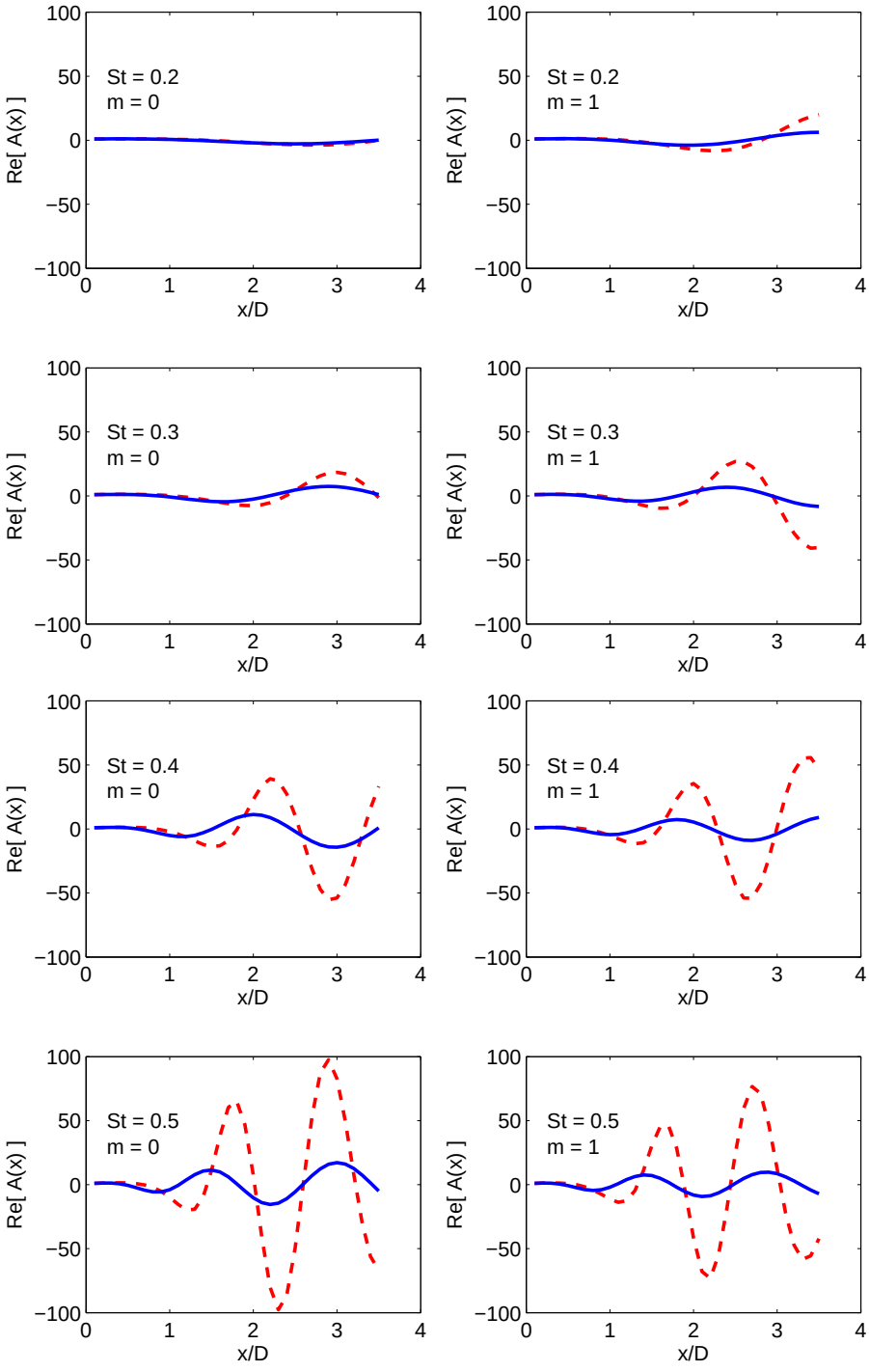

Figure 5. Evolution of spatial amplification factor $A(x) = \exp(i \int^x k(\xi)\, d\xi)$ for the round nozzle `SMC000` (- - - -) and chevron nozzle `SMC001` (———).

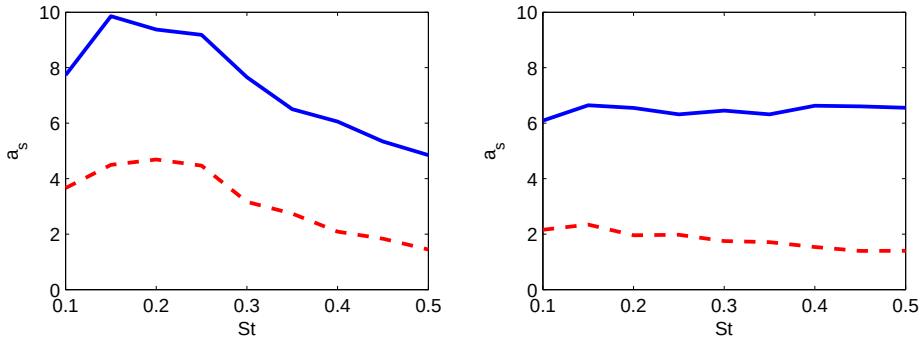

Figure 6. Instability wave amplitude a_i at nozzle exit vs Strouhal number, for the chevron nozzle SMC001 (——), and the round nozzle SMC000 (- - - -). Left/right: $m = 0/m = 1$.

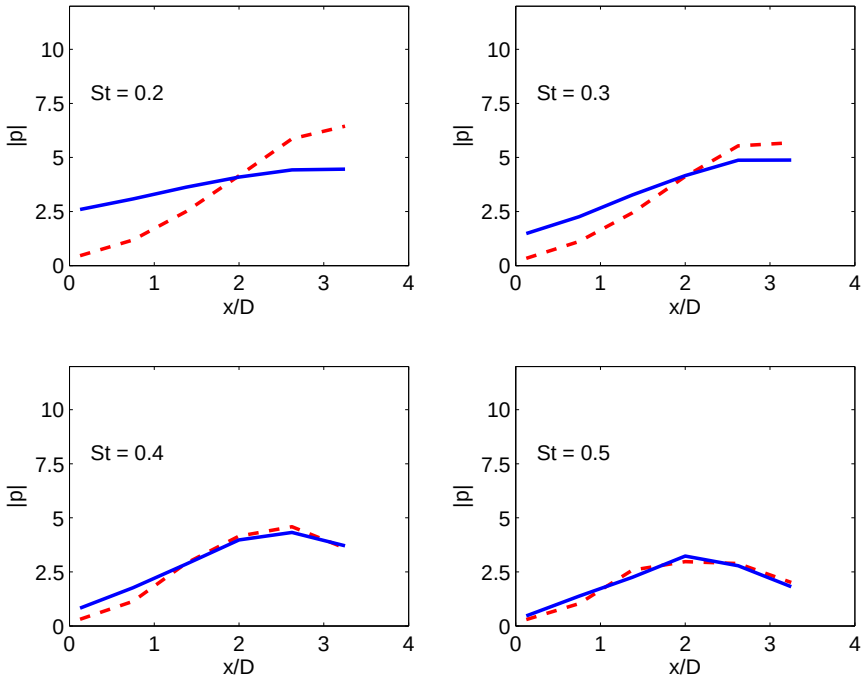

Figure 7. Microphone data (- - - -) and instability wave (——) fit. Nozzle SMC000, $M = 0.5$, $m = 0$.

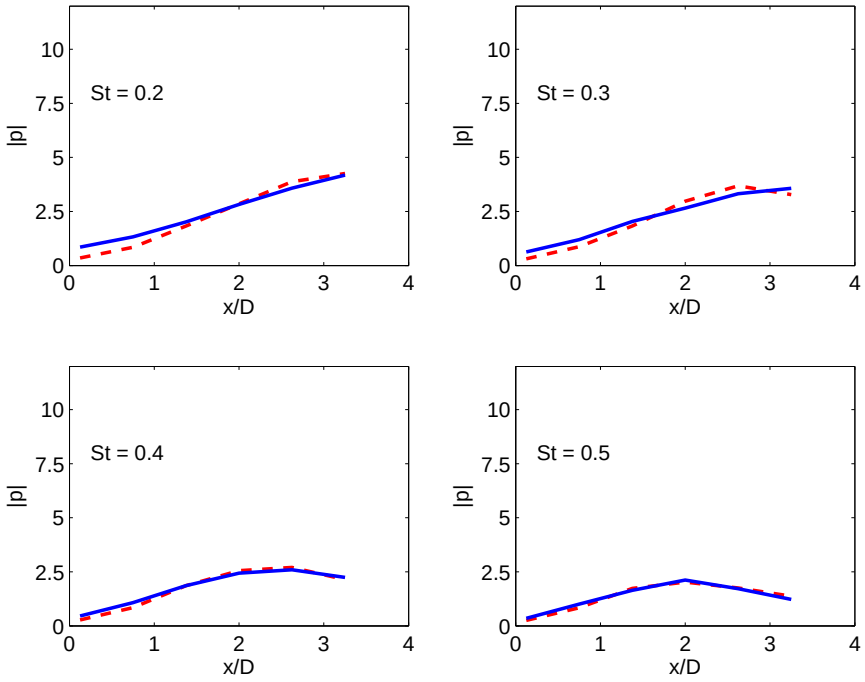

Figure 8. Microphone data (- - - -) and instability wave (———) fit. Nozzle SMC000, $M = 0.5$, $m = 1$.

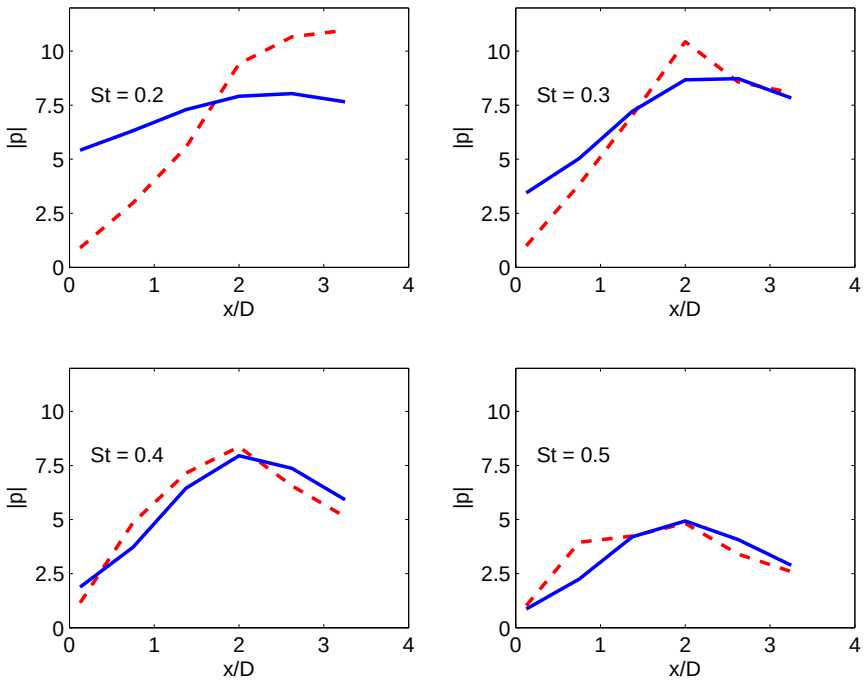

Figure 9. Microphone data (- - - -) and instability wave (———) fit. Nozzle SMC001, $M = 0.5$, $m = 0$.

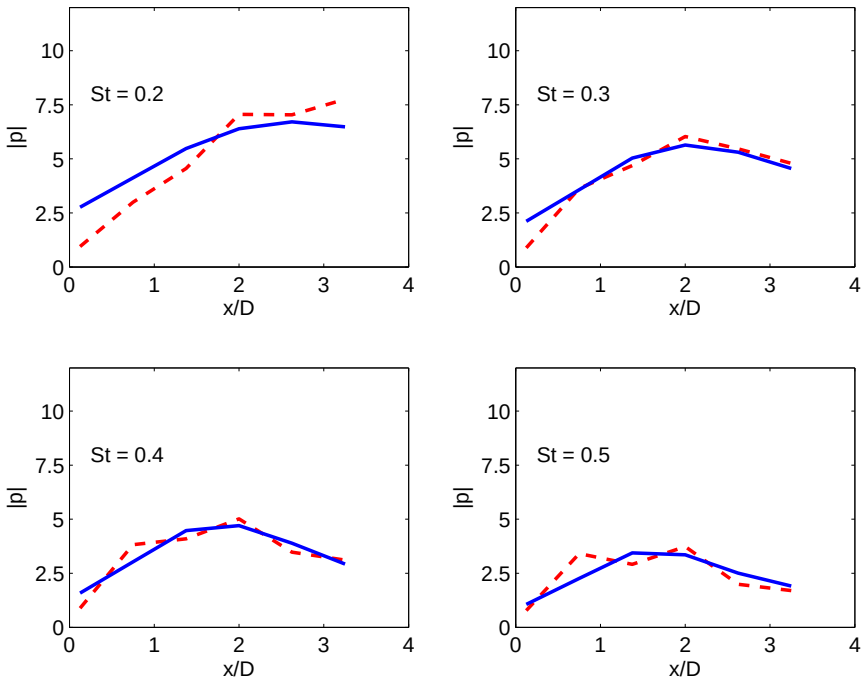

Figure 10. Microphone data (- - - -) and instability wave (———) fit. Nozzle SMC001, $M = 0.5$, $m = 1$.

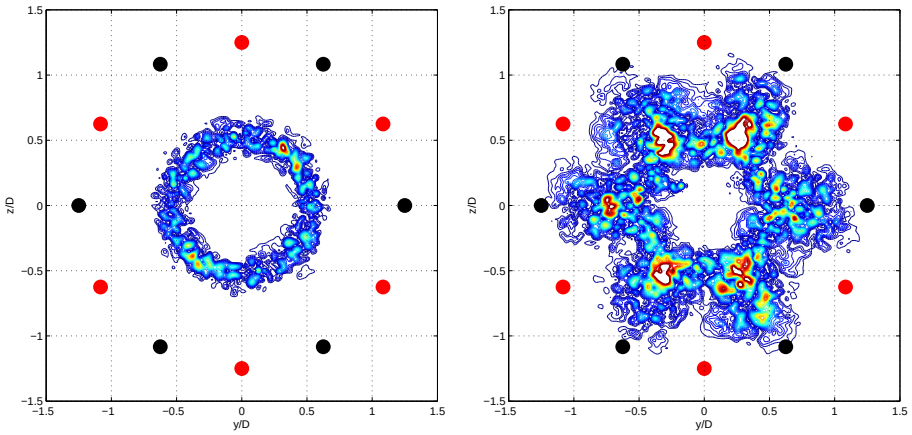

Figure 11. Schematic illustration of proximity effects for a round nozzle (left) and a chevron nozzle (right). Contours show Reynolds stress from PIV data by Bridges et.al.[8] Red dots represent microphone positions on one ring, and black dots represent microphone positions on an adjacent ring. Microphones close to fingers (black) register higher pressure than the ones on the next ring (red), explaining the up-down character of the chevron microphone data.